Acute ischemic stroke thrombi have an outer shell that impairs fibrinolysis

Lucas Di Meglio, Jean-Philippe Desilles, Véronique Ollivier, Mialitiana Solo Nomenjanahary Msci, Sara Di Meglio, Catherine Deschildre, Stéphane Loyau, Jean-Marc Olivot, Raphaël Blanc, Michel Piotin, et al.

Acute ischemic stroke thrombi have an outer shell that impairs fibrinolysis

Lucas Di Meglio MD[1], Jean-Philippe Desilles MD/PhD[1,2], Véronique Ollivier PhD[1], Mialitiana Solo Nomenjanahary MSci[1], Sara Di Meglio MSci[1], Catherine Deschildre MSci[1], Stéphane Loyau MSci[1], Jean-Marc Olivot MD/PhD[3], Raphaël Blanc MD[2], Michel Piotin MD[2], Marie-Christine Bouton PhD[1], Jean-Baptiste Michel MD/PhD[1], Martine Jandrot-Perrus MD/PhD[1], Benoît Ho-Tin-Noé PhD[1†]* and Mikael Mazighi MD/PhD[1,2]*.

[1]Univ Paris Diderot, Sorbonne Paris Cité, Laboratory of Vascular Translational Science, U1148 Institut National de la Santé et de la Recherche Médicale (INSERM), Paris, France.

[2]Rothschild Foundation Hospital, Paris, France. Department of Interventional Neuroradiology.

[3]Toulouse University Medical Center, Toulouse, France

*: both authors contributed equally to this work

Search Terms: Stroke, thrombus histology, thrombus structure, thrombolysis, shell.
Publication history: none

Submission Type: **Article**
Title character count: **75**
Number of Tables : **1 + 1 supplemental**
Number of Figs : **6 + 3 supplemental Figs and 1 video**

Word count abstract : **212**
Word count paper : **3960**

†**Correspondence:**
Benoît Ho-Tin-Noé, PhD.
Laboratory of Vascular Translational Science, U1148 INSERM, 46 rue Henri Huchard 75018 Paris, France. Fax: + 33 (0) 1 40 25 86 02. Tel: + 33 (0) 1 40 25 86 00.
benoit.ho-tin-noe@inserm.fr

Financial Disclosures:

Nothing to report.

Statistical Analysis conducted by Dr. L. Di Meglio, Inserm U1148

Study funding

This work was supported by INSERM, La Fondation pour la Recherche sur les AVC (grant # FR-AVC-003), La Fondation pour la Recherche Médicale (grant #DPC20171138959), Fondation de l'Avenir and by the French Agence Nationale de la Recherche ANR-16-RHUS-0004 (RHU TRT_cSVD), and BPI (CMI2 project TherAVC2.0). Lucas Di Meglio is the recipient of a PhD grant from La Fondation de L'Avenir.

Abstract

Objectives. Thrombi responsible for large vessel occlusion (LVO) in the setting of acute ischemic stroke (AIS) are characterized by a low recanalization rate after intravenous thrombolysis. To test whether AIS thrombi have inherent common features that limit their susceptibility to thrombolysis, we analyzed the composition and ultrastructural organization of AIS thrombi causing LVO**. Methods.** A total of 199 endovascular thrombectomy-retrieved thrombi were analyzed by immunohistology, scanning electron microscopy (SEM), and subjected to *ex vivo* thrombolysis assay. The relationship between thrombus organization and thrombolysis resistance was further investigated *in vitro* using thrombus produced by recalcification of citrated whole blood. **Results.** SEM and immunohistology analyses revealed that, although AIS thrombus composition and organization was highly heterogeneous. AIS thrombi shared a common remarkable structural feature in the form of an outer shell made of densely compacted thrombus components including fibrin, von Willebrand factor, and aggregated platelets. *In vitro* thrombosis experiments using human blood indicated that platelets were essential to the formation of the thrombus outer shell. Finally, in both AIS and *in vitro* thrombi, the thrombus outer shell showed a decreased susceptibility to t-PA-mediated thrombolysis as compared to the thrombus inner core. **Interpretation.** Irrespective of their etiology and despite their heterogeneity, intracranial thrombi causing LVO have a core-shell structure that influences their susceptibility to thrombolysis.

Introduction

Tissue-type plasminogen activator (t-PA) in combination with endovascular therapy (EVT) is the current gold standard for acute ischemic stroke (AIS) recanalization[1]. Until the recent emergence of EVT for large vessel occlusion (LVO) AIS, data on AIS thrombus composition and structure remained scarce. Such information, however, might be highly relevant from a therapeutic perspective.

Among AIS patients with LVO eligible to intravenous t-PA therapy, recanalization is achieved in only approximately 30 % of cases[2,3]. The mechanisms underlying this low response to thrombolytic therapy in LVO are not fully understood, but parameters like thrombus location and size have been shown to influence t-PA delivery and recanalization rates[2–5]. Composition and structure of AIS thrombi could also play an important role in determining their mechanical properties and susceptibility to t-PA-mediated thrombolysis[6–11]. The increased sensitivity of red blood cells (RBCs)-rich coronary thrombi to lysis by t-PA as compared to platelet-rich ones has long been known[12], and *in vitro* studies have shown that thrombus retraction and compaction, as well as higher density and cross-linking of fibrin fibers, confer resistance to t-PA[8,10,13]. Interestingly, immunohistological analyses of thrombi causing LVO have provided converging evidence that those thrombi are highly heterogeneous[14–20]. AIS thrombi contain variable amounts and proportions of RBCs[15,16,21–23], platelets[16,22,23], leukocytes[18,22], fibrin[16,21–23], and von Willebrand factor (VWF)[18,21 19,24]. In addition, recent studies indicate that neutrophil extracellular traps (NETs)are constitutive components of LVO thrombi from all AIS subtypes, and contribute to resistance to t-PA-mediated thrombolysis[19,24]. In fact, NETS-targeting with recombinant DNAse 1 accelerates t-PA-induced *ex vivo* thrombolysis of retrieved AIS thrombi[19,24]. With this as background, we analyzed the composition and ultrastructural organization of LVO thrombi, and investigated how these parameters impact t-PA-mediated thrombolysis.

Methods

Thrombus collection

Patients treated in Rothschild Foundation hospital by EVT from December 2015 to July 2018 with successful thrombi retrieval were enrolled in this study. EVT procedure was chosen at interventionalists' discretion, using a stent-retriever or a direct aspiration first pass technique. AIS thrombi collected at the end of EVT were either fixed for immunohistological analysis or used fresh in *ex vivo* thrombolysis assay.

Standard Protocol Approvals, Registrations, and Patient Consents

Patient information was collected prospectively using a standardized questionnaire (Endovascular Treatment in Ischemic Stroke (ETIS) registry) and are resumed in Table 1. Stroke etiology was classified as described[25]. Human hearts explanted from heart transplant recipients were obtained with the authorization of the French Biomedicine Agency (CODECOH DC2018-3141). The local Ethics Committee approved this research protocol (CPP Nord Ouest II, ID-RCB number: 2017-A01039-44).

Histology and immunostaining

Thrombi fixed 48 hours in 3.7% PFA were embedded longitudinally in paraffin and sectioned at 6 µm. After deparaffinization, antigen retrieval with Tris EDTA pH 9.0 (Target Retrieval Solution, Dako), and blocking with 3 % BSA in PBS, tissue sections were incubated with primary antibodies to fibrinogen (8,5 µg/mL, Dako, ref F011), fibrin (generous gift from Dr. Charles Esmon, Oklahoma Medical Research Foundation, 5 µg/mL, clone 59D8), glycophorin A (6 µg/mL, Dako, clone JC159, M0819), von Willebrandt Factor (15,5 µg/mL, Dako, ref A0082), CD42b (2 µg/mL, Beckman Coulter, ref IM0409), plasminogen activator inhibitor 1

(PAI-1, 15 µg/mL, Merck, MA-33B8), protease nexin-1 (PN-1, 15 µg/ml, gift from D. Hantai, Inserm U1127, Paris, France), or histone H4 citrulline 3 (H4Cit3) (1:200, Millipore, ref 07-596, #2073139), washed 3 times in PBS, and incubated with secondary antibodies either directly conjugated to fluorophores or biotinylated for subsequent amplification with streptavidin-conjugated fluorophores. Tissue sections were finally counterstained with Hoechst 33342 (10 µg/mL, Life Technologies) and mounted in fluorescent mounting medium (Dako). Staining specificity was assessed by omitting the primary antibody on control slices.

Hematoxylin/eosin (H&E) staining was also performed for each AIS thrombus.

For whole mount staining, non-embedded fixed AIS thrombi were washed with PBS, blocked with 3 % BSA in PBS, incubated with the antibodies described above, and counterstained with Syto 64 (5 µM, Life Technologies) and filipin (100 µg/mL, Sigma).

H&E and fluorescent images were acquired using, respectively, a Hamamatsu nanozoomer slide scanner and an Axiovert Zeiss fluorescence microscope equipped with an apotome device.

Measurement of fibrin-rich shell thickness

Thrombus shell thickness was measured on thrombus sections stained in immunofluroescence for fibrin(ogen). Straight line scans perpendicular to the thrombus surface were drawn from edge to edge of thrombus sections, and the width of the 2 fibrinogen fluorescence peaks (one at each extremity of the scan line) was measured. For each thrombus, thrombus shell thickness was defined as the average width calculated from 4 measurements out of 2 line scans. Shell thickness was measured for a total of 118 thrombi.

The mean profile of fibrin distribution in stroke thrombi was determined by averaging edge-to-edge fluorescence intensity profiles along line scans from 6 different thrombi selected randomly. For each thrombus, edge-to-edge distances were normalized to values between 0 and 100, and fluorescence intensity was expressed as a percentage relative to the maximal intensity

value measured along the line scan. All measurements were made using the Zen lite software (Zeiss).

Scanning electron microscopy analysis

Thrombi fixed in 2% glutaraldehyde were cut transversally or longitudinally, and dehydrated by successive immersions in ethanol at increasing concentrations (30%, 50%, 70%, 80%, 90% and absolute ethanol). Dehydrated samples were air-dried in an incubator at 37°C for 2 hours and then sputter coated with gold for 1 minute before scanning electron microscopy (SEM) analysis. SEM images were acquired using a Jeol It 100 scanning electron microscope. Acquisition was made using the secondary electron detector for an acceleration voltage of 10kV and a probe current of 50 pA.

In vitro blood clot formation

Peripheral blood was drawn from healthy donors using Vacutainer citrate tubes (3.2 % buffered sodium citrate, Vacuette) after informed consent was obtained. Clot formation was initiated in glass tubes (Pyrex, 10x75 mm) by recalcification ($CaCl_2$, 16.6 mM) of 250 or 500 µL blood and allowed for 4 hours at 37°C. Thrombi were fixed in 3.7 % PFA for subsequent analysis in SEM.

In a subset of experiments, 30 minutes after recalcification, pre-formed thrombi were transferred in wells of 48-well plates containing 1.5 mL of PBS, PBS supplemented with histones (300µg/mL, Worthington Biochem), PF4 (4µM, R&D System), platelet-poor plasma (PPP), platelet-rich plasma (PRP), or into a suspension of red blood cells (RBCs). After 3.5 hours of incubation in a thermomixer (500 rpm, 37°C), thrombi were either fixed in PFA for analysis in SEM, or used directly in thrombolysis assay. PPP and PRP were obtained by

centrifugation of citrated blood at 2000 x g for 5 minutes and 120 g for 15 minutes, respectively. RBC suspensions were obtained by collecting the pellet of RBCs below the PRP fraction.

In vivo thrombosis

A filter paper (1 × 2 mm) saturated with collagenase P (0.6 mg/mL, Sigma-Aldrich) was applied to the adventitial surface of the carotid artery and removed after 2 min, the artery was immediately rinsed with warm 0.9% saline solution, and a clamp was placed on the collagenase-injured area for 3 min. A red occlusive thrombus formed rapidly after clamp removal and flow restoration in 5 out of 6 carotid arteries subjected to this protocol,

Histone-induced agglutination of red blood cells

Citrated blood drawn from healthy donors was centrifuged 15 minutes at 120 x g. After removal of the PRP, the pellet was resuspended in PBS and centrifuged for 15 minutes at 1200 x g. Pelleted RBCs were finally resuspended in PBS and stimulated with 1 mg/ml calf thymus histones (Worthington Biochem). RBC aggregation was recorded using an Axiovert Zeiss microscope equipped with a color camera (Zeiss).

Thrombolysis assay

For *ex vivo* thrombolysis, thrombi were cut transversally into 2 equal parts, and incubated in 500 µL PBS in the presence or absence of 1 µg/mL of t-PA (Actilyse, Boehringer Ingelheim, Ingelheim am Rhein, Germany) and 1 µM Glu-plasminogen (Technocolone) in a thermomixer (500 rpm, 37°C). Thrombus weight was measured using an ultraprecision balance just before and at 10, 20, 30 and 40 minutes after incubation initiation. Thrombolysis was expressed as a percent relative to baseline thrombus weight.

For thrombolysis of clots produced *in vitro*, clots were left intact or cut in half to expose their core, and the same protocol was used.

Statistical analyses

Data were analyzed using a nonparametric analysis of variance (Kruskal–Wallis) for comparison of more than two groups, or by the Mann–Whitney U-test, for comparison of two groups of unpaired data. Results are presented as median±interquartile range for continuous variables, and as percentages for qualitative variables. The PrismGraph 4.0 (GraphPad Software, San Diego, CA) and Matlab (The Mathwork inc, Natick, Mass) softwares were used. Values of $P<0.05$ were considered statistically significant.

Data Availability

The datasets generated during and/or analysed during the current study are not publicly available but are available from the corresponding author on reasonable request and with permission of all contributing authors.

Results

Intracranial thrombi possess a core-shell structure

Analysis of a subset of 30 AIS thrombi in SEM revealed the presence of a dense, sealed external shell encapsulating a loose erythrocyte-rich core in 24 out of 30 thrombi (Fig 1A to E). Shell components were so densely compacted and agglomerated that they formed a continuous layer, in which individual cells could hardly be detected (Fig 1C and E). This was in stark contrast with the clearly identifiable RBCs, fibrin fibers, and aggregated platelets in the inner core of AIS thrombi (Fig 1D and E).

The presence of an external shell in AIS thrombi was further investigated and characterized in both full thickness whole-mount preparations and sections of AIS thrombi. In agreement with SEM analysis, immunofluorescent staining of fibrin showed a clear difference between the surface and inner core organization of AIS thrombi (Fig 2 and Fig e-1). Whereas fibrin formed a network of individual fibers in the inner core (Fig 2A and D), it formed a sealed network at their surface (Fig 2F-I and Fig e-1).

With respect to cellular components, staining of membrane cholesterol with filipin, a polyene antibiotic that specifically binds to 3-β-hydroxysterols[26], also showed a marked difference between the AIS thrombus core and surface. In the thrombus inner core, cells with well-delineated cell membranes were largely present and easily observed (Fig 2B). At the thrombus surface, intact RBCs were scarce and membrane staining revealed no clear cell border delineation (Fig 2G and Fig e-2). Instead, membrane staining took the form of dense punctuated spots or larger agglomerates, indicative of aggregated platelets and/or cell remains, which was confirmed by positive staining for platelet CD42b and nucleic acids (Fig 2K).

Examination of immunohistological sections confirmed the concentration of thrombus components including fibrin, platelets, leukocytes, VWF, NETs and RBCs in the outermost layer of all 164 AIS thrombi analysed (Fig 3 and Fig e-2).

In contrast to the thrombus surface, the immunohistological appearance of the inner core of AIS thrombi was highly variable from one thrombus to another. The AIS thrombus inner core showed variability in fibrillary and cellular content, both in terms of respective proportion and organization (Fig 3). Although difficult to objectivize, the simplest type of thrombus inner core organization could be depicted as a fairly homogeneous distribution of fibrin and RBCs. A much higher degree of organization was characterized by the presence of inner clusters of platelets, leukocytes, and von Willebrand factor (VWF) from which red blood cells were

excluded and where fibrin fibers were less prominent (Fig 3). Notably, both types of inner core organization could be found within a single given thrombus (Fig 3).

Importantly, to exclude the possibility that the shell observed in AIS thrombi formed secondary to the EVT extraction procedure, we analyzed intracardiac thrombi found in hearts explanted from heart transplant recipients. Like AIS thrombi, intracardiac thrombi showed a compact outer shell in which platelets and fibrin were tightly packed (Fig e-3), thus showing that shell formation in human thrombi can occur irrespectively of EVT procedure.

Taken together, these results indicate that although AIS thrombi are heterogeneous, they share a common feature in the presence of a surface shell that covers and seals part of or the entire thrombus surface.

Fibrin shell thickness is not linked to patient characteristics and treatment

In immunofluorescence, accumulation and compaction of fibrinogen at the thrombus periphery resulted in a fluorescence peak (Fig 4A-B). The width of the fibrinogen fluorescence peak was measured and used to estimate shell thickness in AIS thrombi and to determine its possible correlations with clinical characteristics of AIS patients. There was no difference in thrombus shell thickness between the various etiologies of AIS (Fig 4C, Table e-1). Thrombus fibrin shell thickness was also not different between patients that received t-PA or anti-thrombotic treatment prior to EVT and those who did not (Fig 4D, Table e-1). There was no statistically significant correlation between fibrin shell thickness and major cardiovascular risk factors or other variable such as sex, age, diabetes, tobacco use, site of occlusion, time to recanalization, or clinical outcome (Table e-1).

Platelets are essential to the formation of the thrombus outer shell

We next investigated potential mechanisms underlying outer shell formation in AIS thrombi. We first determined whether the core-shell structure of AIS thrombi was a systematic and inherent feature of blood clots. Analysis in SEM of blood clots formed *in vitro* by recalcification of citrated whole blood showed that, unlike in AIS thrombi, most of the outer surface of these clots was not covered by a shell. In fact, a shell-like external layer where individual cells and fibrin fibers were no longer identifiable was observed only at the upper part of blood clots produced *in vitro* (Fig 5A). With the exception of this top shell-like structure, the clot surface showed clearly distinguishable fibrin fibers and RBCs (Fig 5A). The fact that the shell-like structure was restricted to the clot's upper part indicated an impact of differential cell sedimentation, and thus of cell composition, on its formation. This pointed to a role for platelets, which have the lowest mass density among blood cells, in shell formation. To investigate this possibility, we assessed the ability of platelets and RBCs to induce the formation of a superficial shell around blood clots. Immersing pre-formed blood clots into platelet-rich plasma (PRP) resulted in the formation of a shell covering the entire clot surface and resembling that of AIS thrombi (Fig 5B). In comparison, only a thin superficial layer of fibrin formed when blood clots were immersed into PPP (Fig 5B).

Platelet factor 4 (PF4), which is abundantly stored in platelet alpha granules, has been previously shown to stimulate fusion and agglomeration of fibrin fibers[27]. We thus tested whether purified PF4 or platelet lysates could reproduce the effect of platelets on shell formation. Unlike PRP, neither purified PF4 nor platelet lysates caused the formation of a shell around pre-formed blood clots (data not shown).

We then tested whether RBCs or aggregated RBCs could lead to the formation of a shell-like structure. No shell was observed after immersion of blood clots in a suspension of RBCs. Histones have been recently shown to cause aggregation of RBCs[28]. Although treatment with

extracellular histones caused hemagglutination of isolated RBCs (video 1), it did not cause shell formation at the surface of blood clots (not shown).

Since the mechanisms of shell formation in blood clots formed under static conditions may differ from those involved in thrombosis under flow conditions, we analyzed occlusive thrombi formed *in vivo* in mouse carotid arteries. SEM analysis of occlusive thrombi induced by a combination of mechanical and proteolytic injury to the carotid artery showed that these thrombi had a shell-core structure with a RBC-rich core surrounded by a platelet-rich peripheral shell (Fig 5C). Like in AIS thrombi, fibrin compaction was observed in the latter platelet-rich outer shell, and not in RBC-rich areas (Fig 5C and D).

Altogether, these results indicate that platelets drive shell formation in thrombi, and that platelet granule factors are not sufficient for this function.

The thrombus outer shell is more resistant to t-PA than the thrombus core

Platelets, extracellular DNA, as well as tight assembly and crosslinking of fibrin, as found in the outer shell of AIS thrombi, are well-known to confer resistance to fibrinolysis[19,24,27,29–32]. Staining of AIS thrombi for the platelet-derived direct inhibitors of t-PA, plasminogen activator inhibitor-1 (PAI-1)[33] and protease nexin-1 (PN-1)[34], showed that both PAI-1 and PN-1 were abundant and preferentially accumulated in the platelet-rich outer shell (Fig 6A). SEM analysis of AIS thrombi subjected to *ex vivo* thrombolysis by a cocktail of t-PA and plasminogen showed that the inner core was much more sensitive to thrombolysis than the outer shell (Fig 6B). In fact, after 40 minutes of thrombolysis, while AIS thrombi were emptied of their inner content, their outer shell was still present, giving them the aspect of a donut when observed in cross sections (Fig 6B). The increased resistance to thrombolysis of the outer shell of AIS thrombi indicates that this layer provides a protective coating against thrombolysis. To test this hypothesis, blood clots were treated with PRP to induce the formation of a peripheral shell, and

the rate of thrombolysis of such clots was compared when the clots were left intact or cut in half to breach their shell and expose their inner core. The rate of thrombolysis of intact clots was significantly lower than that of clots with a breach in their external shell Fig. 6C). Importantly, there was no difference in the rate of thrombolysis between intact and cut clots untreated with PRP (data not shown). Taken together, these results show the contribution of the platelet-rich external coating of AIS thrombi to thrombolysis resistance.

Discussion

In the present study, we highlight that AIS thrombi, irrespectively of stroke etiology, share a common structural feature: a dense surface shell encapsulating a highly heterogeneous core.These results are in agreement with our recent observation of a core-shell organization in a thrombus retrieved from an AIS patient[35], and indicate that this thrombus architecture is not an isolated phenomenon but a common one. Remarkably, Ahn *et al.* also noted the presence of an outer shell made of a « fibrin crust » and aggregated platelets in arteriogenic AIS thrombi[36]. Pre-clinical studies in mouse models of hemostasis have suggested the possibility of a core-shell hierarchical organization of hemostatic plugs[37,38], but the clinical existence and relevance of such a thrombus organization in human arterial thrombosis remained to be ascertained.

A major biological and clinical implication of the core-shell structure of AIS thrombi comes from the relative resistance of their shell to t-PA-mediated thrombolysis. In fact, we show that this outer shell made of densely compacted fibrillary and cellular components has a decreased sensitivity to t-PA-mediated thrombolysis as compared to the thrombus inner core, and thus constitutes a shield against t-PA. Our results thus indicate that, besides parameters like thrombus location, length of occlusion, and absence of flow[2–5], thrombus composition and structure also constitute potential barriers to intravenous thrombolysis in AIS patients with

LVO. This thrombus structure-related resistance mechanism may explain in part why even intra-arterial t-PA delivery directly to the thrombus can fail to achieve recanalization in AIS patients[39,40].

Several non-exclusive mechanisms likely contribute to the relative resistance of the AIS thrombus shell to t-PA. We show that shell components are compacted and form a continuous layer in which individual cells and fibrin fibers can hardly be detected. Clot porosity and pressure-driven permeation have been previously shown to determine the rate of drug penetration in thrombi[41]. Therefore, compaction of thrombus components in the shell probably provides a first barrier to t-PA by reducing clot porosity. Notably, *in vitro* studies have revealed that clot retraction and mechanical compaction enhance the antifibrinolytic effect of FXIII-mediated fibrin-fibrin and fibrin-α2-antiplasmin cross-linking[7,8,13]. This process could further add to the thrombolysis resistance of the AIS thrombus shell. The aspect of the fibrin network aspect in the shell suggests that chemical modifications of fibrin also participate in thrombolysis resistance. In fact, in stark contrast to the characteristic fibrous aspect of the fibrin network entrapping RBCs in the inner core, fibrin in the shell had an altered morphology strikingly resembling that of the fibrinolysis-resistant dense matted fibrin deposits produced by various modifications of fibrin, including oxidation[31], carbamylation[30], or exposure to PF4[27]. Besides compaction and modifications of the fibrin network, other biological factors might contribute to increased t-PA resistance in the AIS thrombus shell. In fact, we show that the shell of AIS thrombi also contains factors capable of impairing thrombolysis, such as VWF[21,42], extracellular DNA[19,24], platelets[12], as well as the direct inhibitors of t-PA, PAI-1[43] and PN-1[34]. The presence of those factors in the AIS thrombus shell argues in favor of using adjuvants for improved reperfusion therapies that could benefit AIS of all etiologies.

Targeting non-fibrin shell components might help to open breaches in the shell and thus enhance t-PA efficacy. Our *in vitro* thrombolysis experiments indeed indicate that the integrity

of the outer shell is critical for inhibition of t-PA-mediated thrombolysis, as illustrated by the reduced thrombolysis rate of intact clots compared to clots with a ruptured external shell. In addition to DNAse 1, which was recently shown to improve t-PA action by targeting NETs and extracellular DNA in AIS thrombi[19,24], drugs targeting VWF might as well be worth considering. Pre-clinical studies have shown that recombinant ADAMTS 13, the specific VWF-cleaving protease, and N-acetylcysteine, which breaks up VWF multimers, both have potent thrombolytic activity towards t-PA-resistant thrombi[21,42,44]. Add-on therapies may represent unique opportunities not only to improve recanalization therapy, but also to reduce t-PA doses and the associated risk of intracranial bleeding, which is responsible for an increased mortality rate in t-PA-treated AIS patients[45].

The accumulation of platelets in the thrombus shell, an observation in agreement with that of Ahn *et al.*[36], together with the results of our *in vitro* clotting experiments showing that a core-shell structure could be reproduced by covering blood clots with platelets, but not with RBCs, support the idea that platelets drive AIS thrombus shell formation. Although a peripheral shell was present in almost all LVO thrombi analyzed, shell thickness was highly variable from a thrombus to another. Considering the importance of hemodynamics in blood cell distribution and platelet activation[46–49], variability in AIS thrombus shell thickness and inner core organization might then partly reflect variability in hemodynamic conditions of AIS thrombus formation. The primary site of thrombus formation together with that of embolization and the associated flow turbulences are probably among the factors that determine those conditions and help to shape thrombus architecture and composition, including shell thickness. However, we did not find any correlation between fibrin shell thickness and patient characteristics including stroke etiology, site of occlusion, thrombolytic treatment, or major cardiovascular risk factors. This suggests that isolated parameters like AIS etiology or thrombus localization alone do not

dictate the extent of shell formation. This interpretation should nevertheless be weighed cautiously in regards to the method we used for measuring shell thickness, which was based on fibrin staining-related fluorescence. A yet-to-develop more integrative method taking into consideration other shell components might have given other results. Development of a method for more precise or exact measurement of shell thickness and density represents could help to better understand how the shell of AIS thrombi affects thrombus properties and how it correlates with clinical data. Another limitation of our study comes from the fact that the AIS thrombi we analyzed here were exclusively obtained from patients who did not experience recanalization after t-PA infusion. Therefore, it remains unknown whether AIS thrombi successfully dissolved by t-PA have a shell.

In conclusion, the present study shows that AIS thrombi from patients with LVO share a common core-shell structure, with a relatively t-PA-resistant platelet-rich outer shell made of compacted thrombus components that encapsulates a looser core, whose content and organization is highly heteregenous. Our findings bring new insights in the understanding of AIS thombi and opens new research avenues for the development of novel thrombolytic strategies capable of enhancing lysis of their external shell.

Data available from Dryad (Supplemental Figures e-1-e3, Table e-1, Supplemental Figure and Movie legends)

Appendix 1

Name	Location	Role	Contribution
Lucas Di Meglio, MD	University Paris Diderot, Paris, France	Author	Design and conceptualized study; performed experiments and/or collected data; analyzed data drafted the manuscript for intellectual content; wrote the manuscript
Jean Philippe Desilles MD, PhD	University Paris Diderot, Paris, France	Author	Design and conceptualized study; performed experiments and/or collected data; wrote the manuscript
Véronique Ollivier, PhD	University Paris Diderot, Paris, France	Author	Performed experiments and/or collected data; analyzed data
Mialitiana Solo Nomenjanahary, MSci	University Paris Diderot, Paris, France	Author	Performed experiments and/or collected data;
Sara Di Meglio, MSci	University Paris Diderot, Paris, France	Author	Performed experiments and/or collected data;
Catherine Deschildre MSci	University Paris Diderot, Paris, France	Author	Performed experiments and/or collected data;
Stephane Loyau MSci	University Paris Diderot, Paris, France	Author	Performed experiments and/or collected data;
Jean-Marc Olivot MD, PhD	University of Toulouse, Toulouse, France	Author	Drafted the manuscript for intellectual content
Raphael Blanc, MD	Rothschild Foundation Hospital, Paris, France	Author	Performed experiments and/or collected data;
Michel Piottin, MD	Rothschild Foundation Hospital, Paris, France	Author	Performed experiments and/or collected data;
Marie Christine Bouton, PhD	University Paris Diderot, Paris, France	Author	Provided essential biological tools and reagents, and conceptual advice
Jean-Baptiste Michel MD, PhD	University Paris Diderot, Paris, France	Author	Provided essential biological tools and reagents, and conceptual advice
Martine Jandrot-Perrus MD, PhD	University Paris Diderot, Paris, France	Author	Provided essential biological tools and reagents, and conceptual advice
Benoit Ho-Tin-Noe, PhD	University Paris Diderot, Paris, France	Author	Design and conceptualized study; performed experiments and/or collected data; analyzed data; wrote the manuscript
Mikael Mazighi, MD, PhD	University Paris Diderot, Paris, France	Author	Design and conceptualized study; wrote the manuscript

References

1. Powers WJ, Rabinstein AA, Ackerson T, et al. 2018 Guidelines for the Early Management of Patients With Acute Ischemic Stroke: A Guideline for Healthcare Professionals From the American Heart Association/American Stroke Association. Stroke 2018;
2. Saqqur M, Uchino K, Demchuk AM, et al. Site of arterial occlusion identified by transcranial Doppler predicts the response to intravenous thrombolysis for stroke. Stroke 2007;38(3):948–954.
3. Seners P, Turc G, Maïer B, et al. Incidence and Predictors of Early Recanalization After Intravenous Thrombolysis: A Systematic Review and Meta-Analysis. [Internet]. Stroke 2016;47(9):2409–12.
4. del Zoppo GJ, Poeck K, Pessin MS, et al. Recombinant tissue plasminogen activator in acute thrombotic and embolic stroke. Ann. Neurol. 1992;32(1):78–86.
5. Kamalian S, Morais LT, Pomerantz SR, et al. Clot length distribution and predictors in anterior circulation stroke: Implications for intra-arterial therapy. Stroke 2013;44(12):3553–3556.
6. Weisel JW. Structure of fibrin: Impact on clot stability. J. Thromb. Haemost. 2007;5(SUPPL. 1):116–124.
7. Rijken DC, Uitte De Willige S. Inhibition of Fibrinolysis by Coagulation Factor XIII. Biomed Res. Int. 2017;2017
8. Reed GL, Matsueda GR, Haber E. Platelet factor XIII increases the fibrinolytic resistance of platelet-rich clots by accelerating the crosslinking of alpha 2-antiplasmin to fibrin. Thromb. Haemost. 1992;68(3):315–320.
9. Sabovic M, Lijnen HR, Keber D, Collen D. Effect of retraction on the lysis of human clots with fibrin specific and non-fibrin specific plasminogen activators. Thromb. Haemost. 1989;62(4):1083–1087.
10. Kunitada S, FitzGerald G a, Fitzgerald DJ. Inhibition of clot lysis and decreased binding of tissue-type plasminogen activator as a consequence of clot retraction. [Internet]. Blood 1992;79(6):1420–7.
11. Jang IK, Gold HK, Ziskind AA, et al. Differential sensitivity of erythrocyte-rich and platelet-rich arterial thrombi to lysis with recombinant tissue-type plasminogen activator. A possible explanation for resistance to coronary thrombolysis. Circulation 1989;
12. Jang IK, Gold HK, Ziskind AA, et al. Differential sensitivity of erythrocyte-rich and platelet-rich arterial thrombi to lysis with recombinant tissue-type plasminogen activator. A possible explanation for resistance to coronary thrombolysis. Circulation 1989;79(4):920–928.
13. Rijken DC, Abdul S, Malfliet JJMC, et al. Compaction of fibrin clots reveals the antifibrinolytic effect of factor XIII. J. Thromb. Haemost. 2016;14(7):1453–1461.
14. De Meyer SF, Andersson T, Baxter B, et al. Analyses of thrombi in acute ischemic stroke: A consensus statement on current knowledge and future directions. [Internet]. Int. J. Stroke 2017;0(0):1747493017709671.
15. Brinjikji W, Duffy S, Burrows A, et al. Correlation of imaging and histopathology of thrombi in acute ischemic stroke with etiology and outcome: A systematic review. J. Neurointerv. Surg. 2017;9(6):529–534.
16. Hashimoto T, Hayakawa M, Funatsu N, et al. Histopathologic Analysis of Retrieved Thrombi Associated with Successful Reperfusion after Acute Stroke Thrombectomy. Stroke 2016;47(12):3035–3037.
17. Qureshi MH, Lobanova I, Suri FK, et al. Histopathological characteristics of iv

recombinant tissue plasminogen resistant thrombi in patients with acute ischemic stroke [Internet]. Stroke 2015;46
18. Schuhmann MK, Gunreben I, Kleinschnitz C, Kraft P. Immunohistochemical analysis of cerebral thrombi retrieved by mechanical thrombectomy from patients with acute ischemic stroke. Int. J. Mol. Sci. 2016;17(3)
19. Laridan E, Denorme F, Desender L, et al. Neutrophil extracellular traps in ischemic stroke thrombi. Ann. Neurol. 2017;82(2):223–232.
20. Simons N, Mitchell P, Dowling R, et al. Thrombus composition in acute ischemic stroke: A histopathological study of thrombus extracted by endovascular retrieval. J. Neuroradiol. 2015;42(2):86–92.
21. Denorme F, Langhauser F, Desender L, et al. ADAMTS13-mediated thrombolysis of t-PA-resistant occlusions in ischemic stroke in mice. Blood 2016;127(19):2337–2345.
22. Sporns PB, Hanning U, Schwindt W, et al. Ischemic Stroke: What Does the Histological Composition Tell Us about the Origin of the Thrombus? Stroke 2017;48(8):2206–2210.
23. Niesten JM, Van Der Schaaf IC, Van Dam L, et al. Histopathologic composition of cerebral thrombi of acute stroke patients is correlated with stroke subtype and thrombus attenuation. PLoS One 2014;9(2)
24. Ducroux C, Di Meglio L, Loyau S, et al. Thrombus Neutrophil Extracellular Traps Content Impair t-PA-Induced Thrombolysis in Acute Ischemic Stroke. Stroke 2018;49(3):754–757.
25. Adams HP, Bendixen BH, Kappelle LJ, et al. Classification of subtype of acute ischemic stroke. Definitions for use in a multicenter clinical trial. TOAST. Trial of Org 10172 in Acute Stroke Treatment [Internet]. Stroke 1993;24(1):35–41.
26. Bittman R, Fischkoff S a. Fluorescence studies of the binding of the polyene antibiotics filipin 3, amphotericin B, nystatin, and lagosin to cholesterol. Proc. Natl. Acad. Sci. U. S. A. 1972;69(12):3795–3799.
27. Amelot AA, Tagzirt M, Ducouret G, et al. Platelet factor 4 (CXCL4) seals blood clots by altering the structure of fibrin. J. Biol. Chem. 2007;282(1):710–720.
28. Kordbacheh F, O'Meara CH, Coupland LA, et al. Extracellular histones induce erythrocyte fragility and anemia. Blood 2017;130(26):2884–2888.
29. Boulaftali Y, Lamrani L, Rouzaud M-C, et al. The mouse dorsal skinfold chamber as a model for the study of thrombolysis by intravital microscopy [Internet]. Thromb. Haemost. 2012;107(05):962–971.
30. Binder V, Bergum B, Jaisson S, et al. Impact of fibrinogen carbamylation on fibrin clot formation and stability. Thromb. Haemost. 2017;117(5):899–910.
31. Pretorius E, Lipinski B. Differences in morphology of fibrin clots induced with thrombin and ferric ions and its pathophysiological consequences. Hear. Lung Circ. 2013;22(6):447–449.
32. Pretorius E, Vermeulen N, Bester J, et al. A novel method for assessing the role of iron and its functional chelation in fibrin fibril formation: The use of scanning electron microscopy. Toxicol. Mech. Methods 2013;23(5):352–359.
33. Erickson LA, Ginsberg MH, Loskutoff DJ. Detection and partial characterization of an inhibitor of plasminogen activator in human platelets. [Internet]. J. Clin. Invest. 1984;74(4):1465–72.
34. Boulaftali Y, Ho-Tin-Noe B, Pena A, et al. Platelet protease nexin-1, a serpin that strongly influences fibrinolysis and thrombolysis. Circulation 2011;123(12):1326–1334.
35. Di Meglio L, Desilles JP, Mazighi M, Ho-Tin-Noé B. Thrombolysis-resistant intracranial clot [Internet]. Neurology 2018;90(23):1075–1075.

36. Ahn SH, Hong R, Choo IS, et al. Histologic features of acute thrombi retrieved from stroke patients during mechanical reperfusion therapy. Int. J. Stroke 2016;
37. Stalker TJ, Traxler EA, Wu J, et al. Hierarchical organization in the hemostatic response and its relationship to the platelet-signaling network. Blood 2013;
38. Welsh JD, Poventud-Fuentes I, Sampietro S, et al. Hierarchical organization of the hemostatic response to penetrating injuries in the mouse macrovasculature. J. Thromb. Haemost. 2017;
39. Mazighi M, Meseguer E, Labreuche J, Amarenco P. Bridging therapy in acute ischemic stroke: A systematic review and meta-analysis. Stroke 2012;
40. Rubiera M, Ribo M, Pagola J, et al. Bridging intravenous-intra-arterial rescue strategy increases recanalization and the likelihood of a good outcome in nonresponder intravenous tissue plasminogen activator-treated patients: A case-control study. Stroke 2011;
41. Diamond SL. Engineering design of optimal strategies for blood clot dissolution. Annu. Rev. Biomed. Eng. 1999;1:427–462.
42. Crescente M, Thomas GM, Demers M, et al. ADAMTS13 exerts a thrombolytic effect in microcirculation. Thromb. Haemost. 2012;108(3):527–532.
43. Zhu Y, Carmeliet P, Fay WP. Plasminogen activator inhibitor-1 is a major determinant of arterial thrombolysis resistance. Circulation 1999;
44. De Lizarrondo SM, Gakuba C, Herbig BA, et al. Potent thrombolytic effect of N-acetylcysteine on arterial thrombi. Circulation 2017;
45. Emberson J, Lees KR, Lyden P, et al. Effect of treatment delay, age, and stroke severity on the effects of intravenous thrombolysis with alteplase for acute ischaemic stroke: A meta-analysis of individual patient data from randomised trials. Lancet 2014;384(9958):1929–1935.
46. Fogelson AL, Neeves KB. Fluid Mechanics of Blood Clot Formation [Internet]. Annu. Rev. Fluid Mech. 2015;47(1):377–403.
47. Tangelder GJ, Teirlinck HC, Slaaf DW, Reneman RS. Distribution of blood platelets flowing in arterioles. [Internet]. Am. J. Physiol. 1985;248(3 Pt 2):H318-23.
48. Woldhuis B, Tangelder GJ, Slaaf DW, Reneman RS. Concentration profile of blood platelets differs in arterioles and venules. [Internet]. Am. J. Physiol. 1992;262(4 Pt 2):H1217-23.
49. Turitto VT, Baumgartner HR. Platelet interaction with subendothelium in a perfusion system: Physical role of red blood cells. Microvasc. Res. 1975;9(3):335–344.

Fig Legends

Fig 1. Thrombi from ischemic stroke patients with large vessel occlusion have a shell-core structure. A-E. Representative scanning electron microscopy (SEM) images of thrombi retrieved by thrombectomy from patients with large vessel occlusion (LVO). A shell-core structure, as shown in panels A and E, was found in 24 out of 30 thrombi analyzed by SEM. **A:** Transversal cross-section of a thrombus showing the presence of a dense compacted peripheral layer forming a continuous shell (arrows) encapsulating the thrombus core (asterisk). **B:** Lower magnification view of the surface of another part of the same thrombus highlighting the homogeneous and continuous aspect of the thrombus shell. **C-D**: High magnification views of the shell surface (**C**) and inner core (**D**). Note that, whereas cells and fibrin fibers are clearly identifiable in the thrombus inner core, shell components are so compacted that one can hardly distinguish individual cells or fibers at the thrombus surface. **E:** Image showing the transition from a sealed compact external layer to a much looser core, as was typically found in LVO thrombi.

Fig 2. Comparison of fibrin and cellular component organization between the shell and inner core of thrombi recovered from patients with large vessel occlusion. The organization of the thrombus external shell and inner core was analyzed by immunofluorescent staining of thrombus components in whole mount preparations of thrombi retrieved by mechanical thrombectomy from patients with large vessel occlusion. Thrombus samples were sectioned transversally at mid-length to expose their inner core. **A-J.** Representative images of the thrombus inner core (**A-E**) and shell (**F-J**) organization**.** Panels **A-E** show images of the thrombus inner core, and panels **F-I** show images of the thrombus shell. Fibrin(ogen) immunostaining (green), and staining of cell membrane cholesterol (blue) and nucleic acids (red) with, filipin and syto 64, respectively, strikingly highlight the structural differences between the thrombus inner core (**A-E**) and the shell (**F-J**). Whereas the fibrin forms a network of clearly identifiable fibers in the thrombus core (**D-E**), it appears as densely matted deposits and plates in the shell (**I-J**). Staining of cholesterol and nucleic acids shows that the thrombus core mainly contains cells with classic features of a well-delineated membrane and/or nucleus (white arrow) (**B-E**), while the shell contains punctiform cell aggregates suggestive of platelets and cell fragments (**G-J**). Note that the vast majority of the cellular elements in the shell are positive for nucleic acid staining, thus indicating a leukocyte or platelet, rather than red blood cell, origin. The images shown are representative of whole mount preparations of 8 different thrombi. **K.** En face view of the surface of a thrombus from a patient with large vessel occlusion and stained in whole mount for membrane cholesterol (filipin), nucleic acids and polyphosphates (Syto64), and platelets (CD42b).

Fig 3. **Heterogeneity and common features of thrombi from ischemic stroke patients with large vessel occlusion.** Images of thrombi recovered from 3 different patients are shown in panels **A** to **C**. Note that despite the important heterogeneity in the distribution and proportion of fibrin, VWF, platelets (CD42b), red blood cells (GPA for glycophorin A), and nucleated cells (DAPI) between the different thrombi, the presence of a continuous lining of fibrin and platelets at the thrombus periphery emerges as a common feature of stroke thrombi. Insets show higher magnification views of the squared areas. Bars = 500 µm.

Fig 4. Impact of stroke etiology and intravenous thrombolysis on thrombus shell thickness.

Thrombus sections were stained in immunofluorescence for fibrin(ogen) and shell thickness was estimated by measuring the width of the fibrin(ogen) fluorescence intensity peaks at the thrombus periphery. **A:** Example of a fibrin(ogen) fluorescence intensity profile along an edge-

to-edge line scan through a thrombus section. **B:** Mean fibrin(ogen) fluorescence intensity profile from a thrombus extremity to another. Note the presence of fibrin(ogen) fluorescence intensity peaks at the thrombus periphery, indicating accumulation and compaction of fibrin(ogen) in those areas. This illustrative profile was obtained by averaging the profiles of 6 thrombi selected randomly. The curve shows mean and SEM values. **C:** Comparison of thrombus shell thickness between thrombi from large artery atherosclerosis (LAA), cardioembolic (CE), or undetermined origin. Bars represent medians and interquartile ranges. **D:** Comparison of thrombus shell thickness between patients treated or not with t-PA prior to mechanical thrombectomy. Bars represent medians and interquartile ranges. NS = not significant.

Fig 5. Platelets are essential to clot shell formation. A: The presence of a shell-like structure in blood clots produced *in vitro* by recalcification of citrated whole blood was investigated by scanning electron microscopy (SEM). A several micron-thick dense layer covering the clot surface (arrows) and resembling the shell of acute ischemic stroke (AIS) thrombi causing large vessel occlusion was observed exclusively in the upper part of blood clots produced *in vitro*. **B:** The role of platelets in the formation of the outer shell was investigated by comparing the effect of immersion of pre-formed blood clots in platelet-poor plasma (PPP) or platelet-rich plasma (PRP) on shell formation around those clots. Whereas the surface of pre-formed clots immersed into PRP got covered by a shell-like structure resembling that of AIS thrombi (arrow), only a thin superficial layer of fibrin covered that of clots immersed into PPP (arrowheads). **C.** Scanning electron microscopy images from an occlusive thrombus formed *in vivo* in a mouse carotid artery showing the presence of a surface peripheral layer containing compacted and agglomerated thrombus components surrounding a red blood cell-rich core. The inset in the left panel shows a macroscopic view of the thrombus formed in the carotid artery. The luminal edge of the carotid artery is highlighted in red. **D.** Immunohistological analysis of mouse thrombi shows that the thrombus shell is composed of dense fibrin agglomerated with nucleic acid and polyphosphate-containing cells or cell fragments indicative of platelets and leukocyte fragments. These images are representative of 5 different thrombi.

Fig 6. The shell of acute ischemic stroke thrombi contributes to thrombolysis resistance. **A:** Representative images of fluorescent immunostainings for the direct inhibitors of t-PA, protease nexin-1 (PN-1) and plasminogen activator inhibitor-1 (PAI-1), showing the accumulation of these inhibitors in the shell covering thrombi from patients with large vessel occlusion (LVO) acute ischemic stroke (AIS). **B:** To compare the sensitivity of the shell and inner core parts of thrombi to t-PA-mediated thrombolysis, freshly-retrieved thrombi from AIS patients were transversally cut into 2 equal parts, incubated for 40 minutes in PBS supplemented or not with a thrombolytic mixture of t-PA (1 µg/mL) and Glu-plasminogen (1 µM), fixed in glutaraldehyde, and processed for analysis in scanning electron microscopy (SEM). Representative SEM images obtained for 2 different thrombi are shown. After thrombolysis, thrombi presented with emptied core mass to become hollow shells. These results are representative of a total of 5 independent experiments **C:** Comparison of the thrombolysis rate of blood clots produced *in vitro* with a platelet-rich shell covering their surface, and that were either left intact (■), or cut in half to expose their core (▲). Thrombolysis was quantified by following the thrombus weight change relative to the initial thrombus weight. N = 9 independent experiments. *: $p < 0.05$.

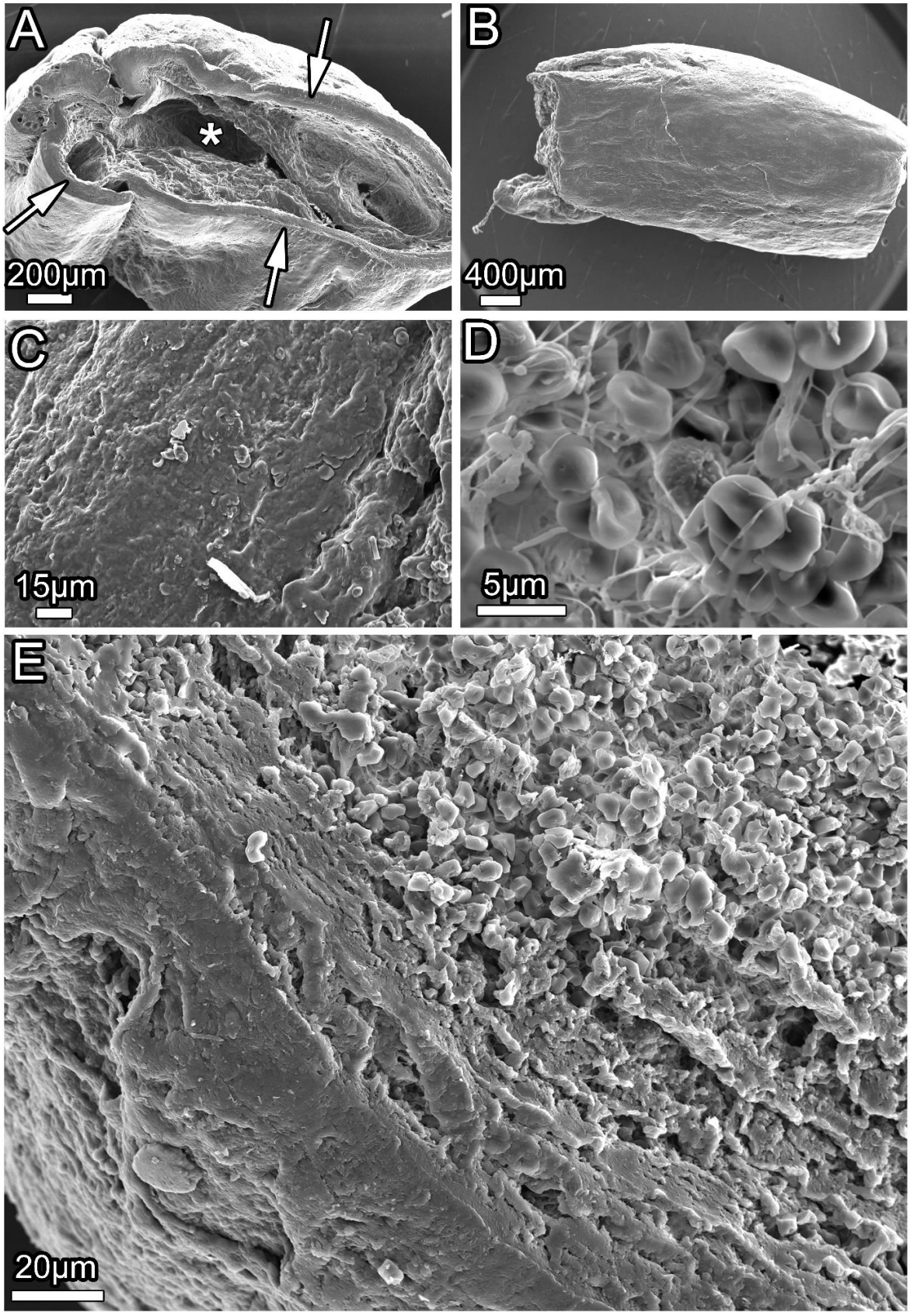

Figure 1

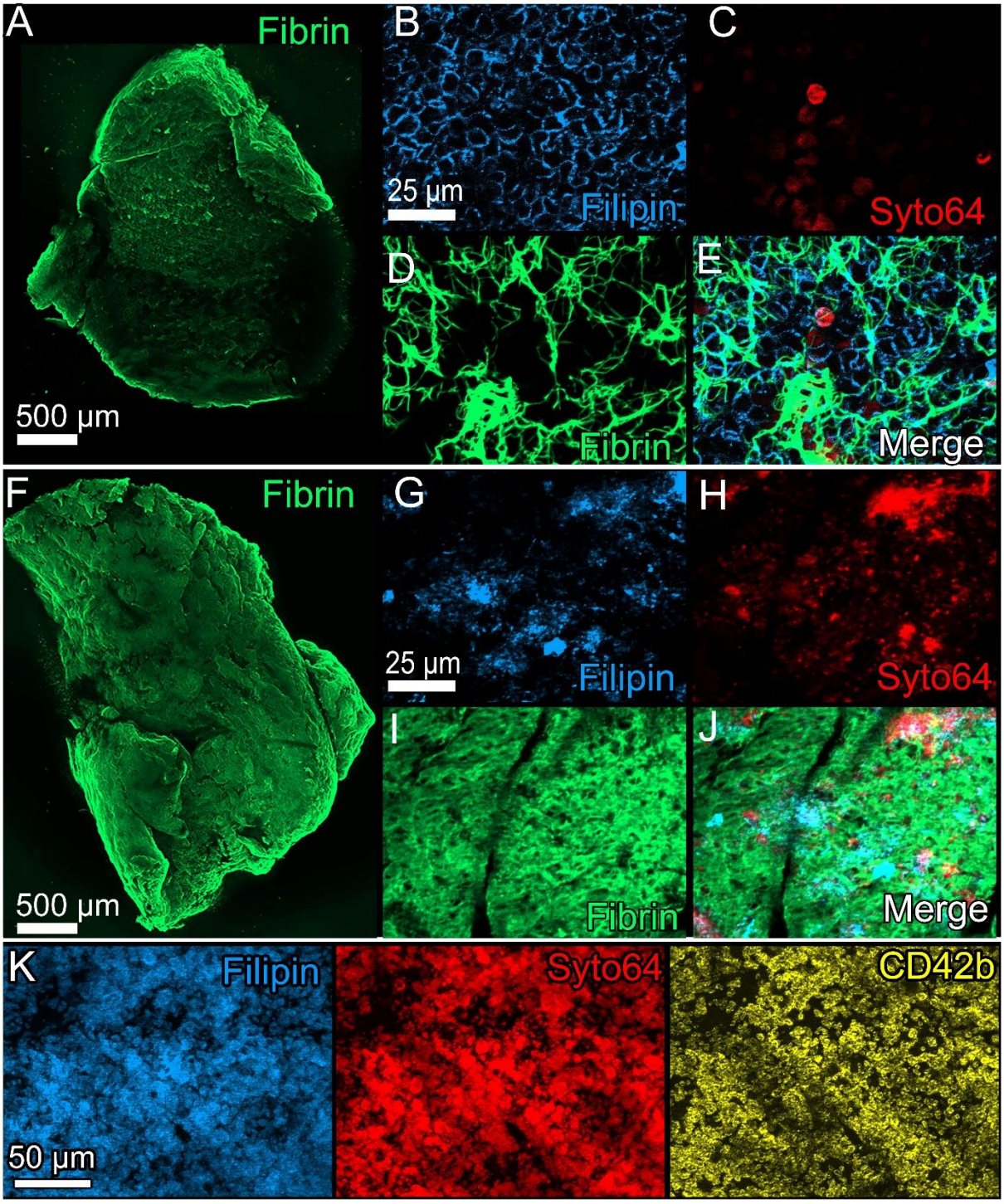
A
Fibrin
500 µm
B
25 µm
Filipin
C
Syto64
D
Fibrin
E
Merge
F
Fibrin
500 µm
G
25 µm
Filipin
H
Syto64
I
Fibrin
J
Merge
K
Filipin
50 µm
Syto64
CD42b

Figure 2

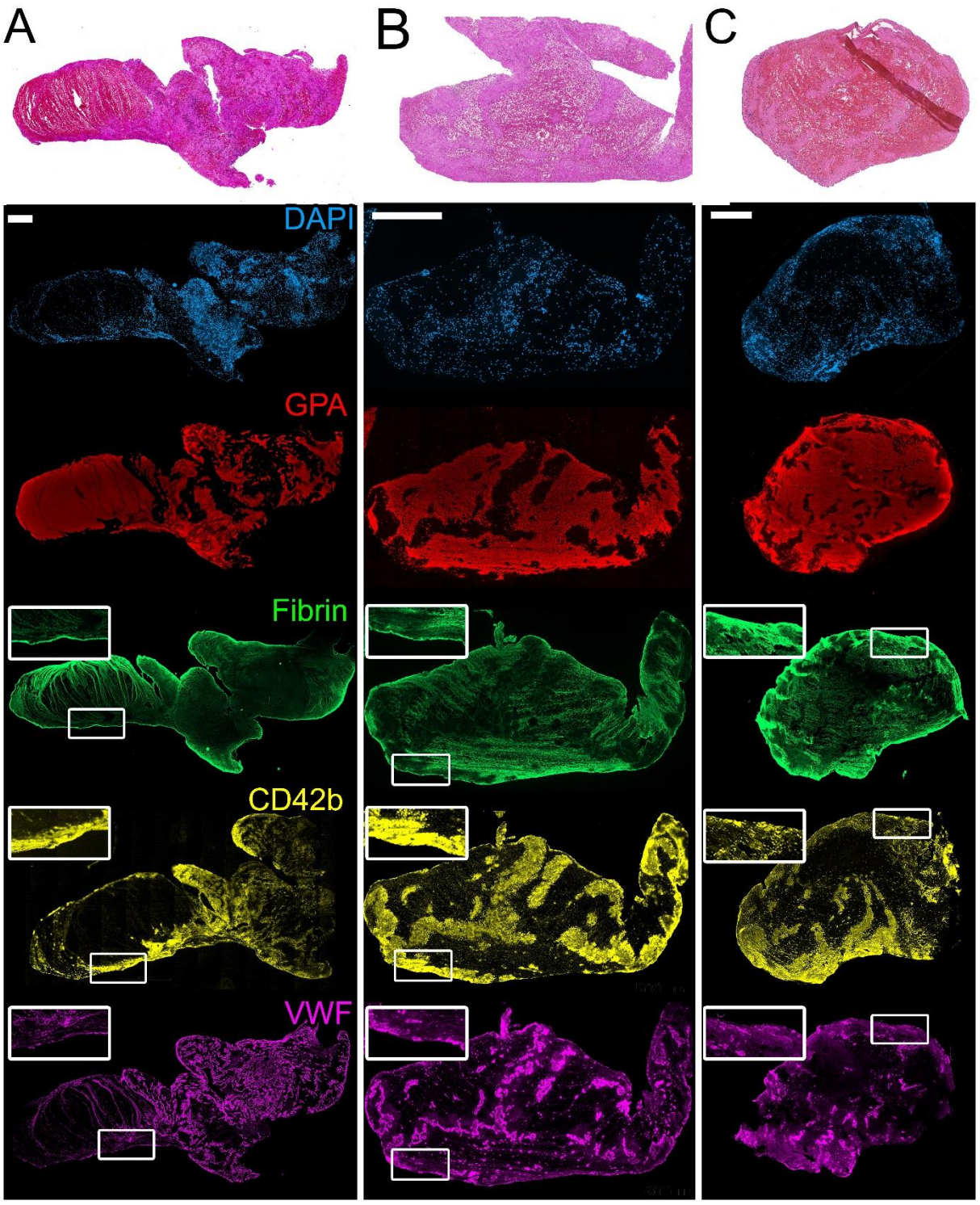

Figure 3

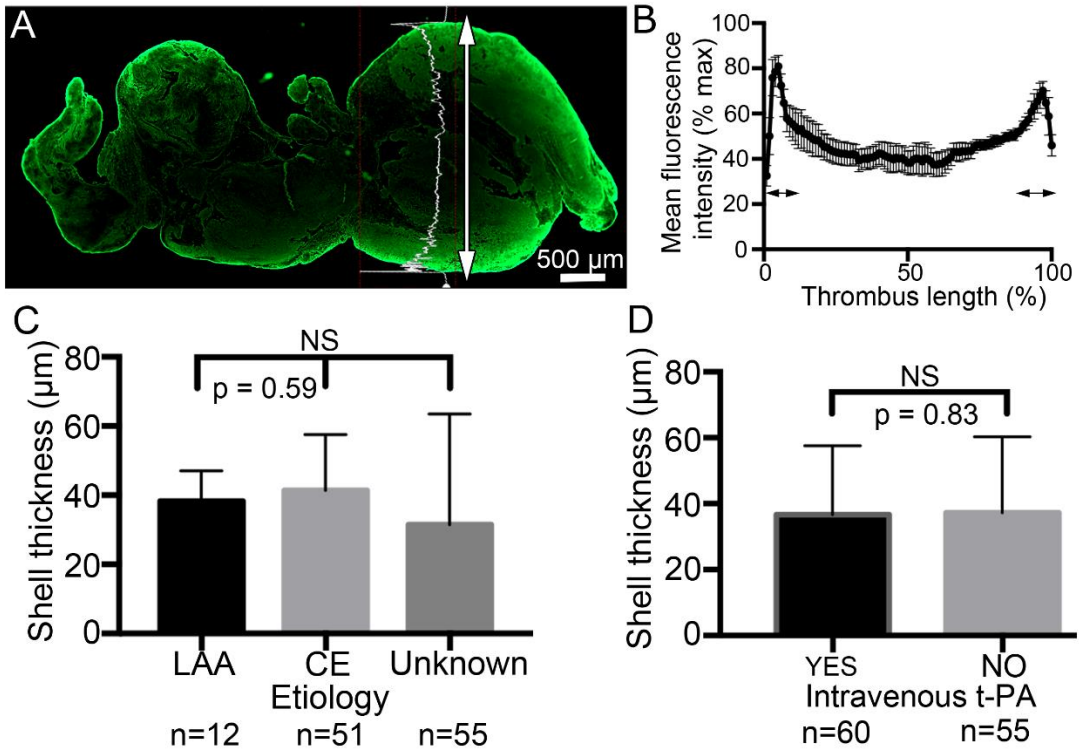
A
500 µm
B
Mean fluorescence intensity (% max)
100
80
60
40
20
0
0
50
100
Thrombus length (%)
C
Shell thickness (µm)
80
60
40
20
0
NS
p = 0.59
LAA
CE
Unknown
Etiology
n=12
n=51
n=55
D
Shell thickness (µm)
80
60
40
20
0
NS
p = 0.83
YES
NO
Intravenous t-PA
n=60
n=55

Figure 4

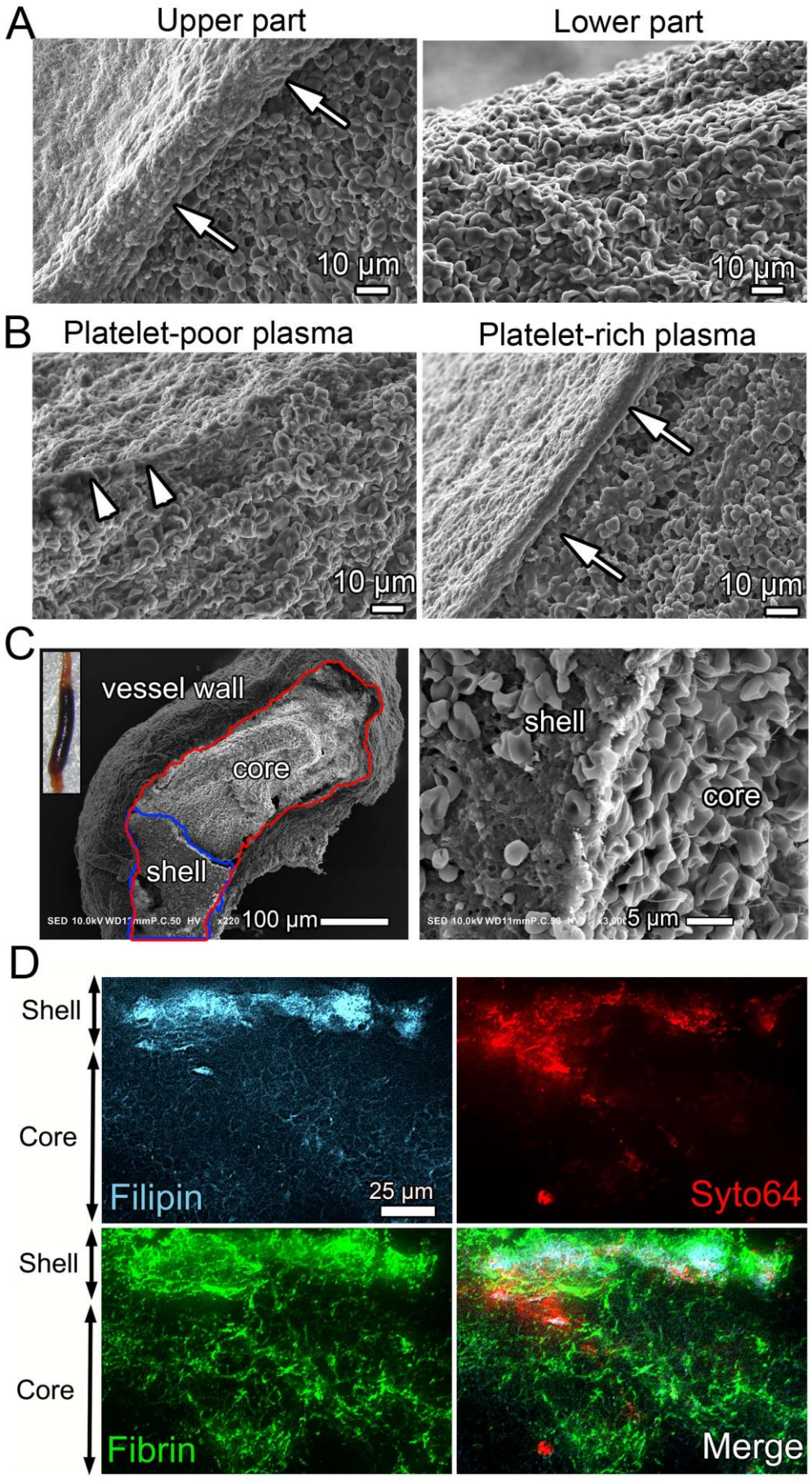
A
Upper part
Lower part
10 μm
10 μm
B
Platelet-poor plasma
Platelet-rich plasma
10 μm
10 μm
C
vessel wall
core
shell
100 μm
shell
core
5 μm
D
Shell
Core
Filipin
25 μm
Syto64
Shell
Core
Fibrin
Merge

Figure 5

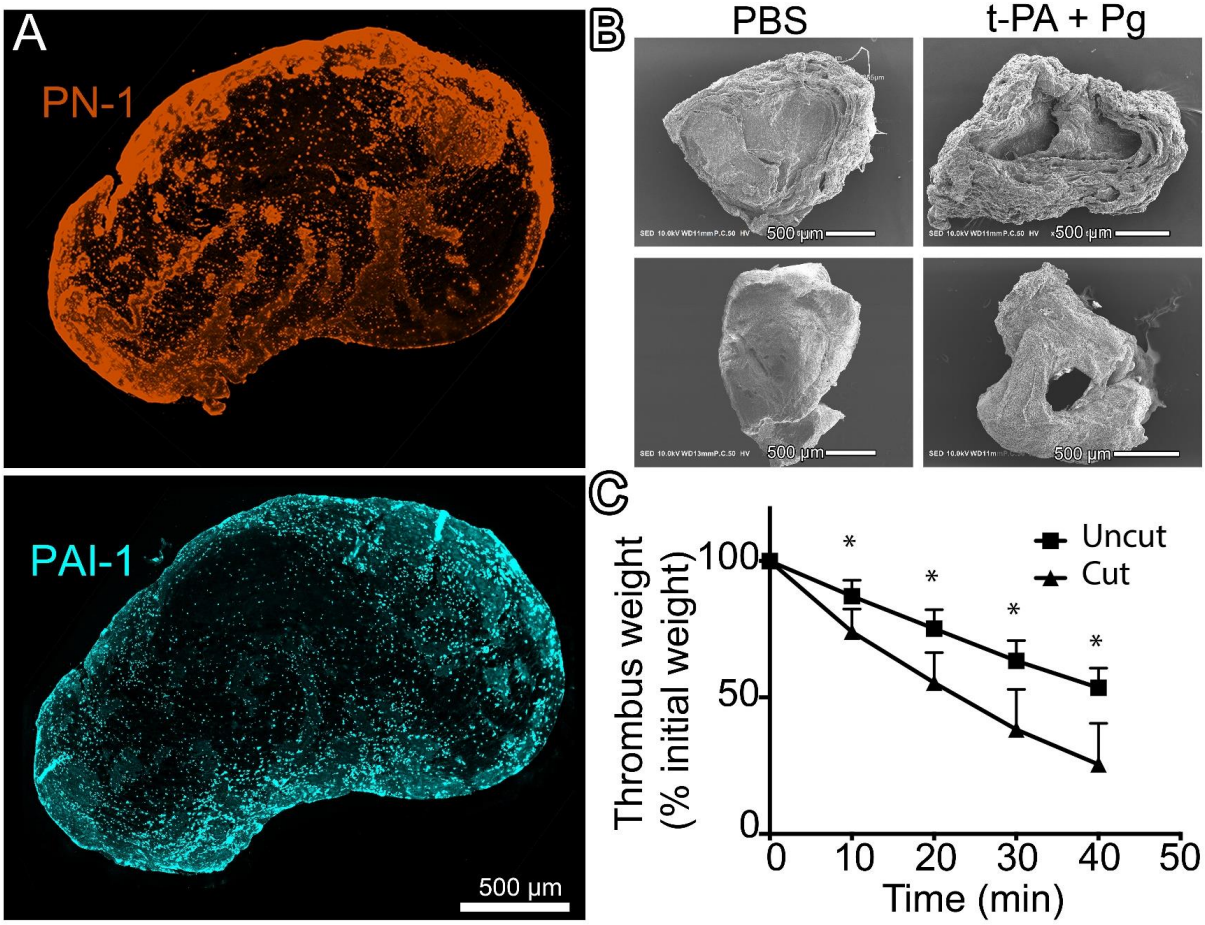
A
PN-1
PAI-1
500 µm
B
PBS
t-PA + Pg
500 µm
500 µm
500 µm
500 µm
C
Thrombus weight
(% initial weight)
100
50
0
0
10
20
30
40
50
Time (min)
Uncut
Cut
*
*
*
*

Figure 6